Evaluation of Scheduling Algorithms under Mobility in a Realistic Ray-Traced Wireless Network

Onem Yildiz, *Aydin Adnan Menderes University*

***Abstract*— Efficient scheduling and link adaptation mechanisms are essential for ensuring reliable and high-throughput communication in mobile wireless networks, particularly in the context of future 6G systems. This study investigates the performance of three prominent scheduling algorithms—Round Robin (RR), Best Channel Quality Indicator (Best-CQI), and Proportional Fair (PF)—in a realistic ray-traced wireless environment under user mobility. A time-evolving scenario is designed where mobile users follow predefined trajectories, and the downlink transmission is evaluated in terms of effective Signal-to-Interference-plus-Noise Ratio (SINR), spectral efficiency, and achieved Transport Block Error Rate (TBLER). Link adaptation is implemented via an Outer Loop Link Adaptation (OLLA) mechanism that dynamically adjusts the modulation and coding scheme based on feedback. The results show that PF scheduling achieves a balanced trade-off between throughput and fairness, maintaining spectral efficiency close to the Shannon capacity while satisfying the target BLER for all users. In contrast, Best-CQI provides high spectral efficiency for strong users but degrades the performance of users with weaker channel conditions. RR ensures fairness but suffers from throughput inefficiencies under dynamic SINR variations. The study highlights the importance of scheduler selection in mobility-aware systems and demonstrates how OLLA-driven adaptation improves robustness in realistic, time-varying channels.**

***Index Terms*— 6G, Link Adaptation, Ray Tracing Simulation, Scheduling, User Mobility.**

I. INTRODUCTION

Future wireless communication systems, especially in architectures moving towards 6G, aim to simultaneously optimize performance metrics such as link reliability and spectral efficiency. To achieve this goal, many technical components such as channel-aware resource allocation, link adaptation, and flexible scheduling strategies for mobile users need to be considered together [1, 2]. In this context, the time-variation of channel conditions experienced by mobile users in multiple access environments directly affects both the link quality and the efficient utilization of system resources. Therefore, scheduling of users in a channel quality sensitive manner should be considered together with link adaptation techniques.

Link adaptation is a Layer-2 mechanism that maximizes data rate while keeping the error rate low by dynamically adjusting transmission parameters according to channel conditions. Outer Loop Link Adaptation (OLLA) [3], a prominent link adaptation technique, tries to compensate for non-idealities in channel estimates by dynamically correcting the Modulation and Coding Scheme (MCS) selection based on the targeted block error rate (BLER) [4]. However, the performance of OLLA directly depends on how the scheduling algorithm allocates users based on channel quality. There are significant differences between schedulers such as Round Robin (RR), Proportional Fair (PF) and Channel Quality Indicator (CQI)-aware scheduling in terms of resource allocation fairness, spectral efficiency and error rates [5, 6].

Recent comparative studies have begun to address these mobility-related trade-offs more explicitly. Fan et al. propose a mobility-aware joint user-scheduling and resource-allocation scheme that minimizes end-to-end latency in federated-learning networks spanning multiple base stations, underlining how scheduler choice can dominate QoS when users move rapidly between cells [7]. Deng and Blough extend this idea to mmWave WLANs, showing that proactive, mobility-predicted schedulers can outperform conventional reactive policies in both capacity and fairness when channel conditions evolve on the order of seconds [8].

In order to develop systems that can adapt to variable environmental conditions in the real world [9, 10], it is of great importance to realistically model scenarios in simulation environments. For this purpose, the simulation frameworks used to evaluate such mechanisms at the system level are also important. Sionna, NVIDIA's open-source physical layer simulation library, enables realistic link adaptation tests with both detailed channel modeling and PHY abstraction mechanisms [11]. This platform enables the generation of coverage maps at the physical layer [12], the simulation of channel performance based on the time-varying location of users, and the measurement of spectral efficiency based on performance key metrics such as path gain, Received Signal Strength (RSS) and Signal-to-Interference-plus-Noise Ratio (SINR). Furthermore, the effect of link adaptation on the system can be compared with the Shannon capacity to analyze how close the system is to the theoretical limits [13].

In contrast to many existing studies which focus on static users or consider the scheduling and link adaptation

Onem Yildiz is with the Department of Electrical and Electronics Engineering, Faculty of Engineering, Aydin Adnan Menderes University, 09100, Aydin, Türkiye. (e-mail: onem.yildiz@adu.edu.tr).

mechanisms in isolation [14-17], in this work, the impact of link adaptation on scheduling algorithms using ray tracing simulations is systematically studied in terms of effective SINR, spectral efficiency and TBLER performance metrics in a dynamic network characterized by user mobility. The performance of OLLA when used with different scheduling algorithms is shown in comparison with the theoretical Shannon capacity. This demonstrates in detail how the impact of scheduling strategies affects not only the resource allocation efficiency but also the behavior of link adaptation in a dynamic wireless network.

In the remainder of the study, section 2 presents the system model and simulation infrastructure, section 3 presents the simulation results and discussion, section 4 presents conclusions.

II. System Model and Methodology

This work meticulously examines the efficacy of schedulers responsible for link adaptation and resource allocation within the time-frequency domain in a multi-user cellular communication context. The system is constructed utilizing the physical layer simulation architecture of the Sionna library and channel modeling supported by ray tracing [18]. The subsequent sections present the system components, physical layer abstraction, and simulation flow in a comprehensive manner.

A. Channel Model and Physical Environment

In this study, a single-cell wireless communication scenario is modeled, comprising one fixed-position base station and three mobile users traversing predefined linear trajectories. Each user is equipped with a single antenna, while the base station is configured with multiple antennas equal in number to the active users, enabling spatially distinct communication links.

The simulation environment includes dynamic user locations over time to see how user mobility affects link quality. To ensure realistic propagation modeling, common construction materials listed in ITU-R P.2040-2 [19] were explicitly parameterized; relative permittivity and conductivity values for concrete, brick, metal, and ground surfaces were assigned. A high-fidelity ray tracing simulation records the environment's propagation characteristics and creates a spatial distribution map of SINR values across the coverage area. Figure 1 shows that the base station is marked with a red dot and the three users' starting points are marked with orange dots. The black lines show the paths that the users can take to move in a straight line during the simulation. The color-coded background illustrates the SINR distribution in the environment, where lighter regions represent higher signal quality, and darker areas indicate zones of weaker reception due to obstruction and shadowing effects caused by surrounding buildings.

This SINR map allows the simulation to extract the instantaneous link quality corresponding to the real-time user position at each transmission interval. These SINR values are used as input to link adaptation and scheduling algorithms to reflect realistic performance under mobility.

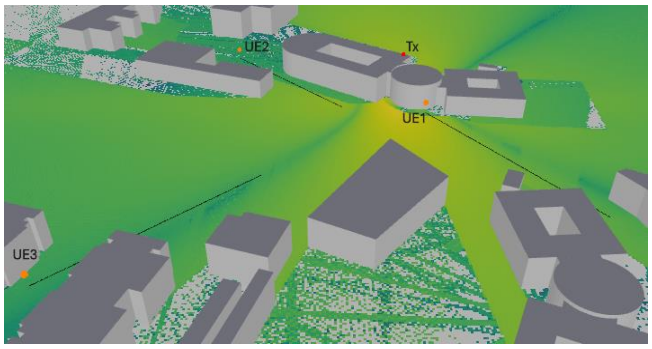

Fig. 1. Map representation in Sionna

In this study, SINR is calculated based on received signal power, interference and thermal noise as follows:

$$SINR_{i,j}^{k} = \frac{RSS_{i,j}^{k}}{N_0 + \sum_{k' \neq k} RSS_{i,j}^{k'}} \quad (1)$$

where $RSS_{i,j}^{k}$ represents the received signal power for the kth user at the ith subcarrier and jth time sample, and N_0 represents the thermal noise power.

The slot-wise SINR values are summarized across time-frequency sources to calculate the effective SINR ($SINR_{eff}$) for each user. $SINR_{eff}$ is a scalar quantity that models the average error behavior of coded symbols when they are subjected to different SINRs in the time, frequency or stream dimensions with a single SINR value in the AWGN channel. In this way, the BLER (Block Error Rate) observed under variable channel conditions can be reproduced under a constant channel model.

Effective SINR is calculated as follows:

$$SINR_{eff} = -\beta \left(\frac{1}{N} \sum_{i=1}^{N} e^{-SINR_i/\beta} \right) \quad (2)$$

where $SINR_i$ is the instantaneous SINR value observed for each time-frequency source $i = 1, \ldots, N$, N is the total number of resource units (number of subcarriers times number of slots), and β is a positive parameter that depends on the MCS used. This metric is used in this study to summarize the SINR distributions of time-moving users under different scheduler algorithms (Round Robin, Best-CQI, Proportional Fair) into a single value. In particular, in the OLLA-based link adaptation process, these $SINR_{eff}$ values are used as direct input for MCS selection.

B. Time-Frequency Resource Structure

The simulation utilizes a time-frequency grid including 128 subcarriers and 12 OFDM symbols per slot, with a spacing of 30 kHz for a slot duration of 0.5 ms. User mobility is modeled throughout 200 slots by updating positions and reassessing channels, facilitating dynamic resource allocation according to real-time link quality. Each user can be allocated multiple

subcarriers per slot, determined by the scheduling rules and channel state information. Slot-specific SINR values are utilized to determine appropriate MCS levels and achievable data rates, creating a direct correlation between channel dynamics, resource allocation, and link adaptation.

C. Link Adaptation

Link adaptation is a mechanism that selects the appropriate Modulation and Coding Scheme (MCS) taking into account changing channel conditions, thus aiming for reliable communication and optimized spectral efficiency. In this study, we use OLLA, one of the link adaptation techniques, to steer the system below the targeted BLER value of 0.1. To achieve this, MCS decisions are based on HARQ feedback and update the channel estimates according to the offset values (μ) shown in (3).

$$\mu_{n+1} = \mu_n + \Delta_n \; ; \Delta_n = \begin{cases} +\alpha, if\ HARQ = NACK \\ -\beta, if\ HARQ = ACK \end{cases} \quad (3)$$

In (3), α and β denote upward/downward step sizes, respectively. The ratio between α and β determines the average BLER that the OLLA converges to (4) [20]. Thanks to this control mechanism, OLLA adapts to changes in link quality over time and keeps the data transmission performance at the targeted level.

$$BLER_{target} = \frac{\beta}{\alpha+\beta} \quad (4)$$

To highlight OLLA's convergence behavior within the limited 200-slot window, the step pair has been fixed at α = 1 dB and β = 0.11 dB, which corresponds to the 0.1 BLER target (=10%). With this relatively large upward step size, the offset reaches steady state in only a few HARQ rounds, allowing the simulation to demonstrate how each scheduler interacts with a fully settled OLLA loop rather than its transient phase. Although smaller steps would yield smoother steady-state ripple, they would require substantially more slots to converge and thus obscure the main scheduler-level effects we wish to compare.

Within the scope of the study, spectral efficiency values were obtained by using the OLLA technique and compared with the Shannon capacity (5) of the system specified as theoretical limit.

$$C = B \log_2(1 + SINR) \quad (5)$$

The system structure described above allowed for a comparative analysis of the impact of different scheduling algorithms on both link quality and link adaptation performance. In the next section, the technical structures of these scheduling algorithms are described in detail.

D. Scheduling Algorithms

Resource allocation is a critical element that directly affects the performance of wireless communication systems. For this reason, this study comparatively evaluates the performance of Round Robin (RR), Proportional Fair (PF) and Best-CQI scheduling algorithms that are frequently used in literature.

Round Robin algorithm is an algorithm that does not care about the channel quality experienced by users, but only about fairness between users. In each slot, one user is allocated resources, and this procedure is repeated across all users.

Best-CQI is an algorithm that allocates resources to the user with the highest channel quality in each slot. While this approach improves overall system efficiency, it negatively affects inter-user fairness by limiting access to resources for users with lower channel quality.

The Proportional Fair (PF) scheduler provides a decision mechanism that balances channel gain and user fairness. In each slot n, the user with the highest relative gain is selected by calculating the ratio of the user's estimated data rate $R_k(n)$ and the historical average data rate $T_k(n)$ as in (6). The decision rule is defined as follows:

$$k^*(n) = \arg max_k \left(\frac{R_k(n)}{T_k(n)}\right) \quad (6)$$

The average rates are updated over time with an exponentially weighted average as in (7):

$$T_k(n+1) = \left(1 - \frac{1}{\tau}\right) T_k(n-1) + \frac{1}{\tau} R_k(n) \quad (7)$$

where $1/\tau \in (0,1)$ is a constant factor [21]. This structure enables users who have been operating at low rates for an extended period to acquire priority in the future, as well as users who have good channel conditions to efficiently utilize system resources.

The contents described in this section have been adapted to our network scenario with Sionna ray tracing simulations using the values specified in Table I. The next section presents the simulation results in detail.

TABLE I
SIMULATION PARAMETERS

Parameter	Value
Carrier frequency	3.5 GHz
# of subcarriers	128
Subcarrier spacing	30 kHz
# of OFDM symbols	12
# of slots	200
Transmitter power	44 dBm
# of BS	1
# of BS antenna/user	1
# of users	3
Target BLER	10%
α	1 dB
Schedulers	RR, Best-CQI, PF
Number of reflections	8

III. RESULTS AND DISCUSSION

A. Impact of Scheduling Algorithms on Effective SINR

Figure 2, Figure 3, and Figure 4 show the time series of effective SINR values observed for each user under different scheduling algorithms. The Round Robin (Figure 2) exhibits a structure where users are assigned to slots sequentially regardless of channel quality. Therefore, users with low SINR (e.g., user 2) often consume system resources, which reduces the overall average SINR and prevents the system from efficiently utilizing the channel gain.

According to the Effective SINR graphs obtained under the Best-CQI scheduling algorithm as shown in Figure 3, the determining effect of the physical location of the users on the channel quality is clearly visible. User 1, which has the advantage of Line-of-Sight (LoS) on the path closest to the transmitter, communicated with a constant and high effective SINR value in the range of 29-30 dB in almost all slots. While user 2 initially received no resource, it became active and prioritized by the algorithm when the channel conditions improved and the SINR level reached 29 dB. On the other hand, user 3 only received resources in a few slots as it followed a path with more signal blocking and severe shadowing, and the effective SINR in these slots remained between 18 dB-23 dB. These results show that the Best-CQI algorithm consistently prioritizes users with high SINR regions, thus increasing system capacity but reducing service continuity for users in poor channel conditions.

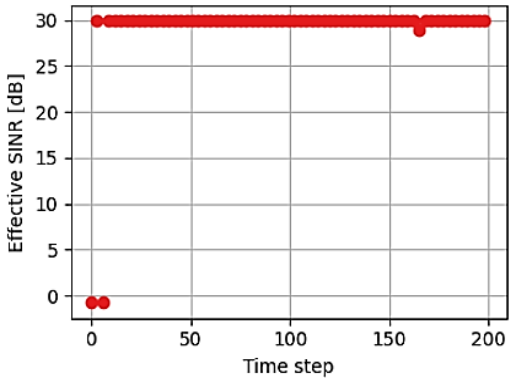

(a) Effective SINR of user 1

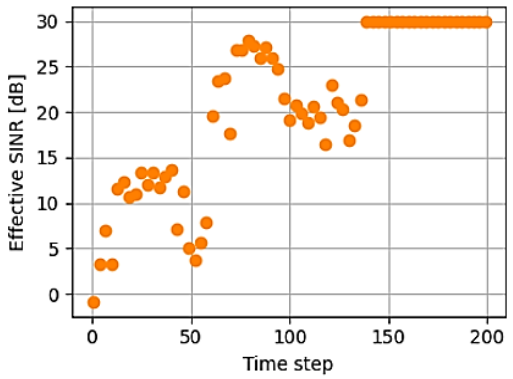

(b) Effective SINR of user 2

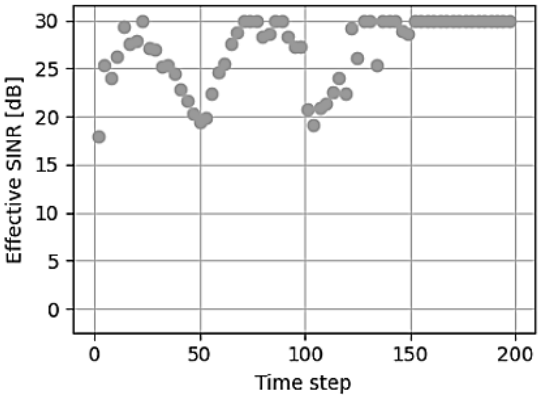

(c) Effective SINR of user 3

Fig. 2. Effective SINR values for RR Scheduler

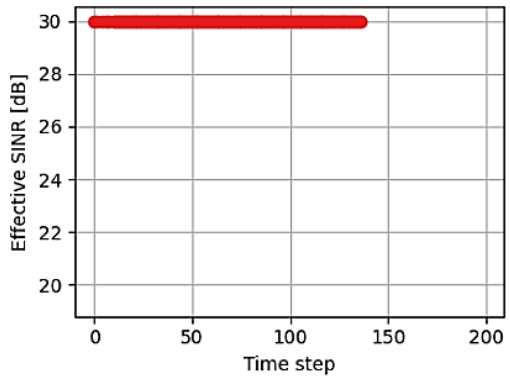

(a) Effective SINR of user 1

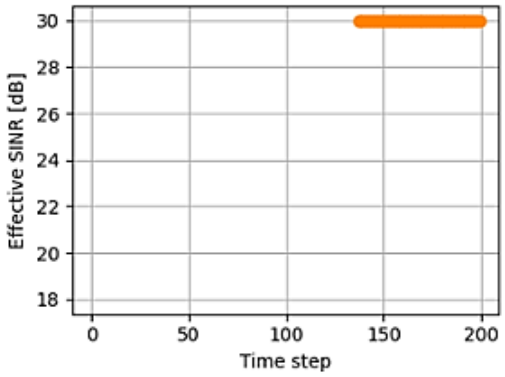

(b) Effective SINR of user 2

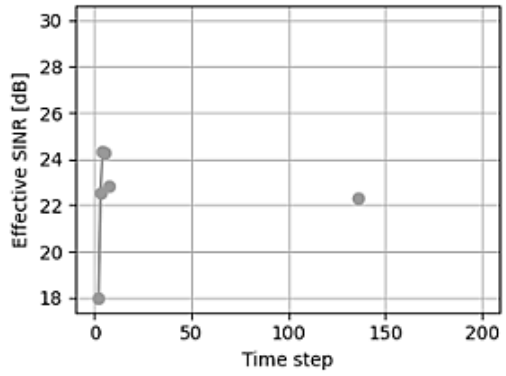

(c) Effective SINR of user 3

Fig. 3. Effective SINR values for Best-CQI Scheduler

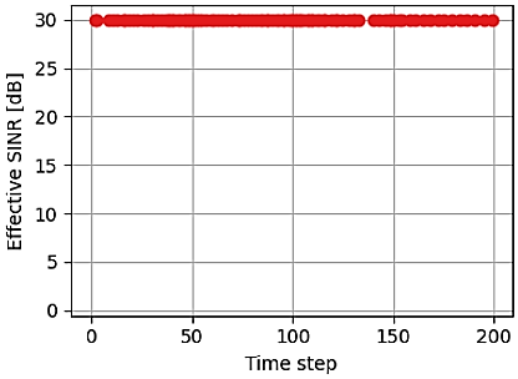

(a) Effective SINR of user 1

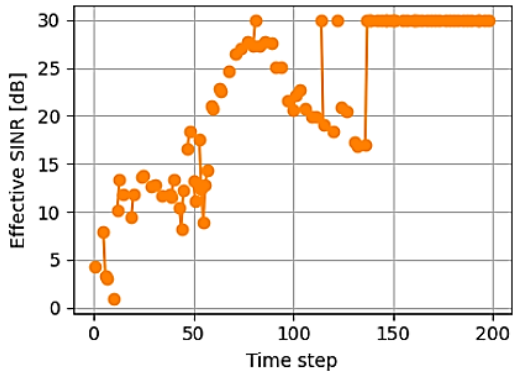

(b) Effective SINR of user 2

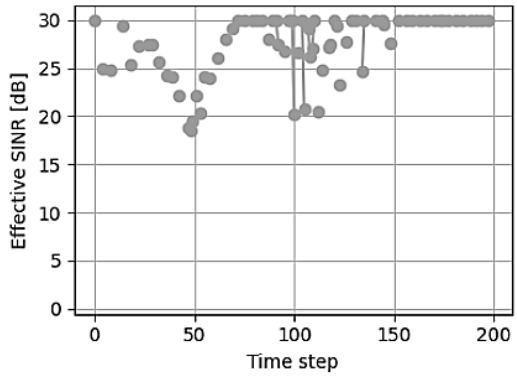

(c) Effective SINR of user 3

Fig. 4. Effective SINR values for PF Scheduler

Figure 4 shows the results of the PF algorithm. According to the effective SINR graphs, user 1's channel conditions remain constant over time, and it receives continuous resource allocation with high SINR values (~30 dB) due to the presence of a direct LoS along the user's path. User 2's SINR values fluctuate significantly over time, ranging from 5 dB to 30 dB. This indicates exposure to building shadowing and multipath effects during movement. User 3 mostly operates at high SINR levels; however, occasional drops indicate possible temporary movement along low SINR regions. Because the PF aims to provide every user with an opportunity, user 2 is allocated resources during periods of low SINR, which increases the variance of the SINR.

B. Impact of Scheduling Algorithms and OLLA on Achievable Spectral Efficiency

Figure 5, Figure 6, and Figure 7 show the spectral efficiency values of the users over time. In each graph, the theoretical Shannon capacity curve is also presented to evaluate the closeness of the link adaptation in practice to the theoretical limit. Under the Round Robin algorithm (Figure 5), spectral efficiency fluctuates significantly and then shows a recovery over time with OLLA adaptation. Due to the sequential resource allocation to all users, low SINR users often transmit data with low MCS levels, which limits the overall system capacity.

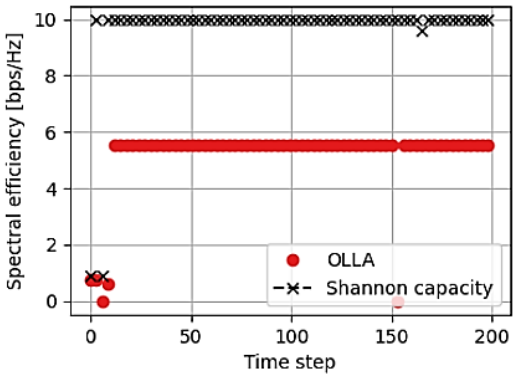

(a) Spectral efficiency of user 1

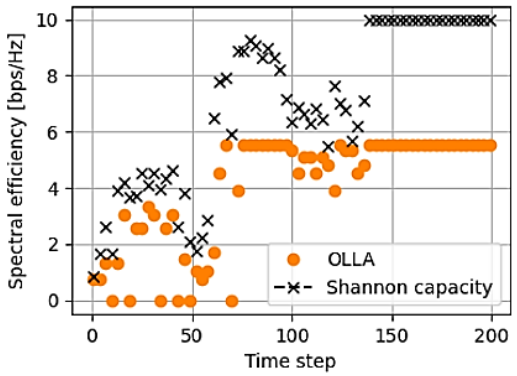

(b) Spectral efficiency of user 2

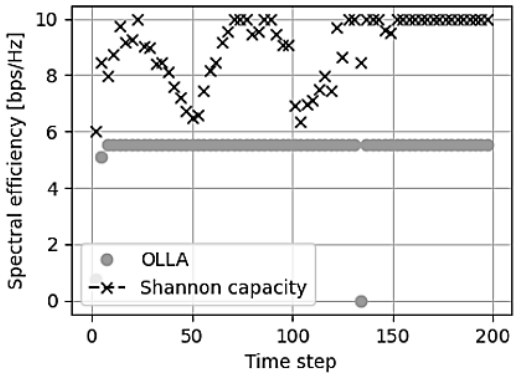

(c) Spectral efficiency of user 3

Fig. 5. Spectral efficiency values of users for RR Scheduler

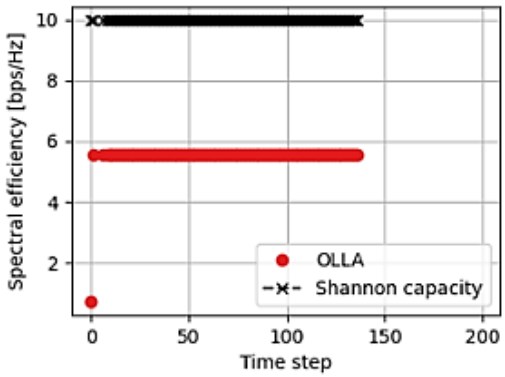

(a) Spectral efficiency of user 1

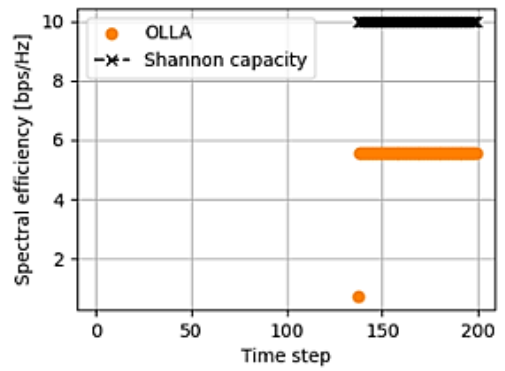

(b) Spectral efficiency of user 2

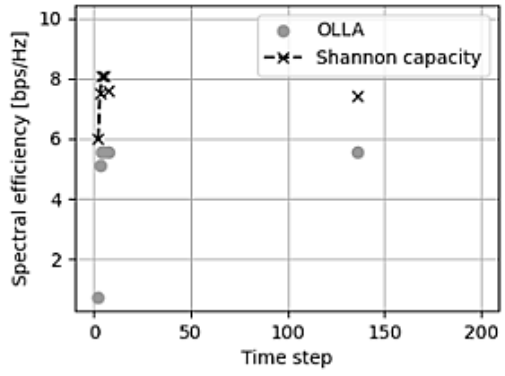

(c) Spectral efficiency of user 3

Fig. 6. Spectral efficiency values for Best-CQI Scheduler

The spectral efficiency values of users under the Best-CQI scheduler (Figure 6) reflect their spatial differences, which are directly related to channel quality. Considering the map in Figure 1, it can be seen that user 1, which has the LoS advantage, benefits from resource allocation for the longest period of time and is served with high efficiency. User 2, initially characterized by poor channel conditions, is eventually seen to benefit from resource allocation, partially reaching higher SINR regions. On the other hand, user 3 travels through lower SINR regions along its path and is matched with resources in only a limited number of slots, achieving at most a short-term spectral efficiency of around 6 bps/Hz.

The results obtained under the Proportional Fair algorithm (Figure 7) show that the selected MCS levels, especially for users 1 and user 3, are very close to the system capacity. Despite the sudden changes in the channel conditions of user 2, the system seems to be stable thanks to the MCS adjustments made by the OLLA algorithm.

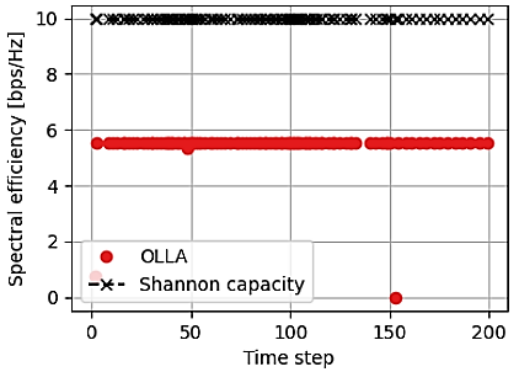

(a) Spectral efficiency of user 1

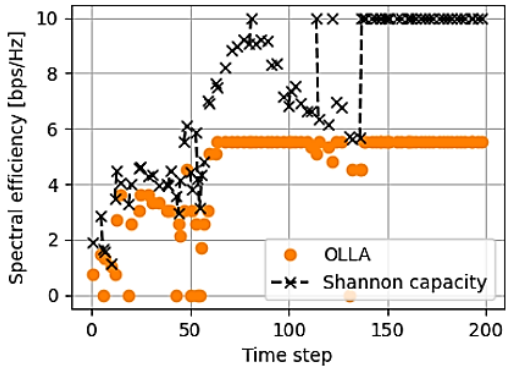

(b) Spectral efficiency of user 2

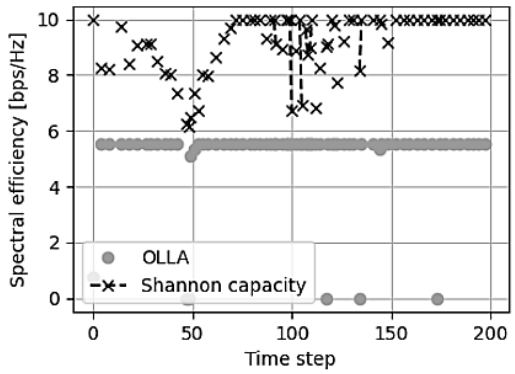

(c) Spectral efficiency of user 3

Fig. 7. Spectral efficiency values for PF Scheduler

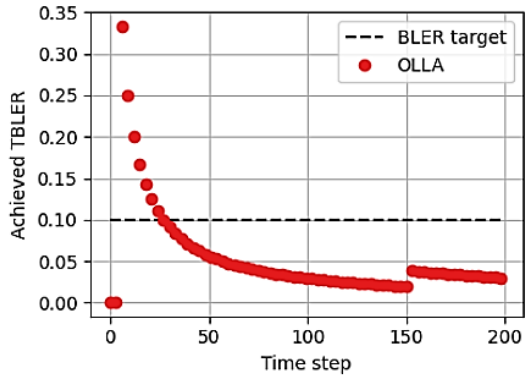

(a) Achieved TBLER of user 1

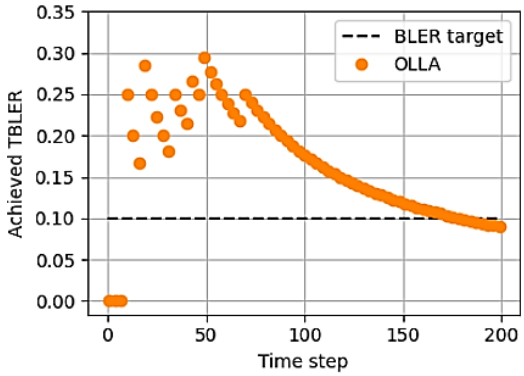

(b) Achieved TBLER of user 2

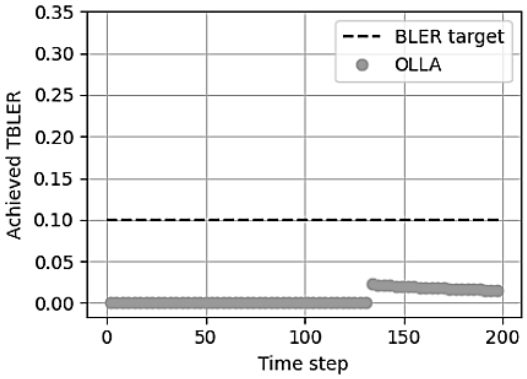

(c) Achieved TBLER of user 3

Fig. 8. Achieved TBLER values for RR scheduler

C. Impact of Scheduling Algorithms and OLLA on Achieved TBLER

Figure 8, Figure 9 and Figure 10 present the TBLER values obtained for each scheduler algorithm separately. In the case of the RR algorithm (Figure 8), TBLER values were observed to be well above the target at times, and OLLA's balancing capacity was strained due to more frequent slot allocation, especially to users with low channel gain.

The TBLER plots obtained under the Best-CQI scheduler show that the OLLA mechanism operates at values well below the target TBLER threshold of 0.1 for all users (Figure 9). In particular, the TBLER values for user 1 and user 2 are close to zero, while user 3, which receives a limited number of resource allocations, similarly achieves very low error rates. This shows that the system successfully maintains reliability despite aggressive MCS selection under high SINR conditions.

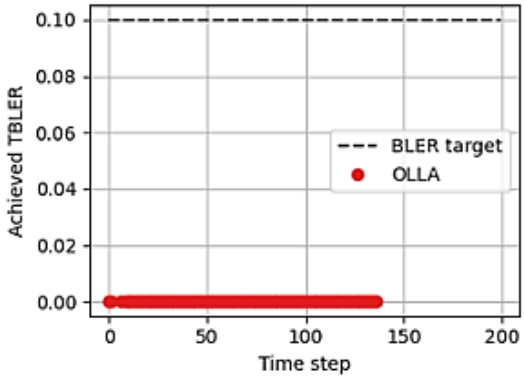

(a) Achieved TBLER of user 1

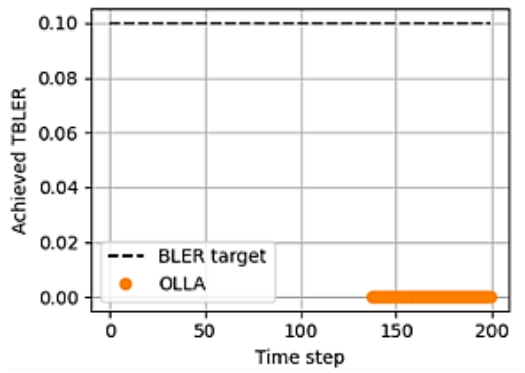

(b) Achieved TBLER of user 2

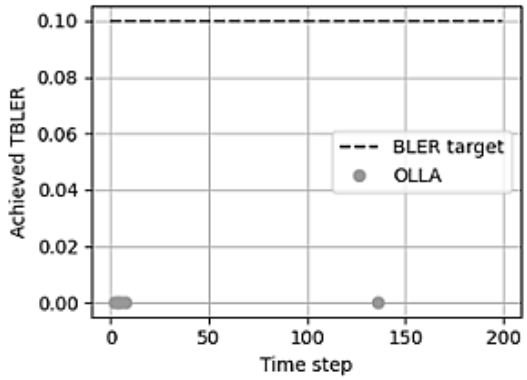

(c) Achieved TBLER of user 3

Fig. 9. Achieved TBLER values for Best-CQI Scheduler

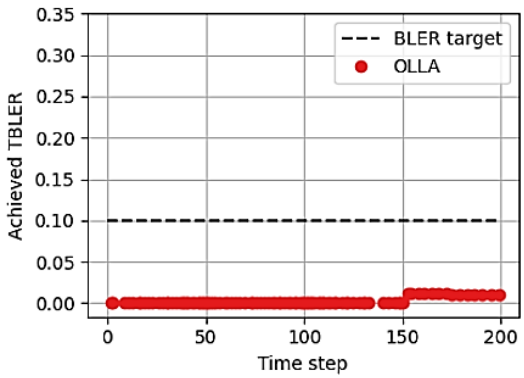

(a) Achieved TBLER of user 1

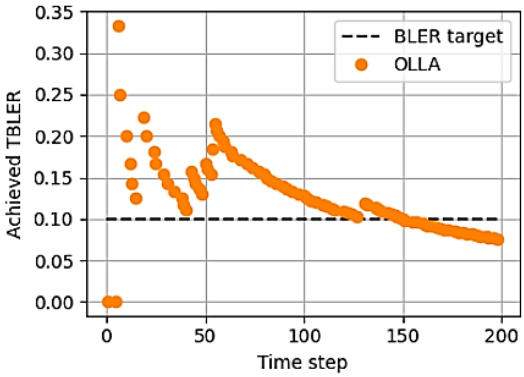

(b) Achieved TBLER of user 2

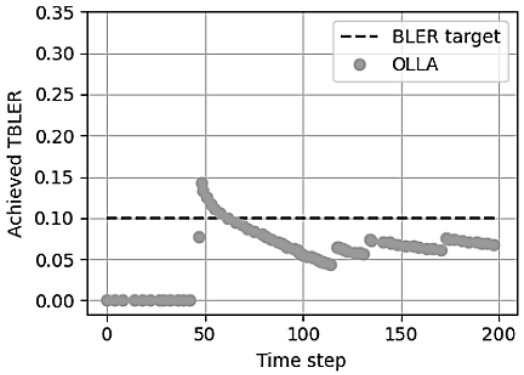

(c) Achieved TBLER of User 3

Fig. 10. Achieved TBLER values of users for PF Scheduler

Under the PF algorithm (Figure 10), the TBLER values fluctuate steadily around the 10% target, while OLLA reacts quickly and successfully maintains the target level.

Table II, Table III, and Table IV present the statistical analysis of SINR, spectral efficiency (SE), and Transport BLER (TBLER) for the RR, Best-CQI, and PF schedulers, respectively, reporting the mean, standard deviation, 95% confidence interval (CI), and sample count for each user.

Results in Table II show that the time-fair RR scheduler gives user 1 and user 3 average SINR values of 29.1 dB and 27.0 dB, with corresponding spectral efficiencies of 5.18 and 5.40 bps/Hz, respectively; however, the weaker user 2 transmits at only 20.6 dB SINR and 4.08 bps/Hz, pushing its TBLER up to 13% and lowering the cell-wide averages.

TABLE II
PERFORMANCE METRICS STATISTICAL ANALYSIS FOR ROUND ROBIN

User	Metric	Mean	Std. Dev.	95% CI	Samples
User 1	SINR [dB]	29.11	5.12	[27.86, 30.36]	67
	SE [bps/Hz]	5.18	1.35	[4.85, 5.50]	67
	TBLER	0.05	0.04	[0.04, 0.06]	67
User 2	SINR [dB]	20.57	8.72	[18.44, 22.69]	67
	SE [bps/Hz]	4.08	1.97	[3.60, 4.56]	67
	TBLER	0.13	0.05	[0.12, 0.14]	67
User 3	SINR [dB]	27.03	3.55	[26.16, 27.90]	66
	SE [bps/Hz]	5.40	0.90	[5.18, 5.62]	66
	TBLER	0.01	0.01	[0.00, 0.01]	66

In Table III, the Best-CQI strategy maximizes capacity by focusing on the two strongest users: both user 1 and user 2 operate at a constant 30 dB SINR with spectral efficiencies of about 5.5 bps/Hz and virtually zero TBLER, whereas user 3 is scheduled in just six slots and achieves 22.4 dB SINR together with 4.68 bps/Hz—an extreme illustration of the throughput–fairness trade-off.

Table IV places PF squarely between these extremes. It retains the 30 dB SINR and 5.50 bps/Hz performance of user 1 while still assigning 97 slots to user 2, raising its average SINR to 21.1 dB and spectral efficiency to 4.13 bps/Hz; the cost is a moderate mean TBLER of 15 % for that user, only slightly above the 10 % target. Altogether, PF alleviates the starvation observed with Best-CQI while avoiding the pronounced efficiency loss of RR, emerging as the most sustainable scheduler for balancing high aggregate capacity, acceptable error rates, and improved user fairness.

TABLE III
PERFORMANCE METRICS STATISTICAL ANALYSIS FOR BEST-CQI

User	Metric	Mean	Std. Dev.	95% CI	Samples
User 1	SINR [dB]	30.00	0.00	[30.00, 30.00]	132
	SE [bps/Hz]	5.52	0.42	[5.45, 5.59]	132
	TBLER	0.00	0.00	[0.00, 0.00]	132
User 2	SINR [dB]	30.00	0.00	[30.00, 30.00]	63
	SE [bps/Hz]	5.48	0.61	[5.33, 5.63]	63
	TBLER	0.00	0.00	[0.00, 0.00]	63
User 3	SINR [dB]	22.39	2.232	[19.95, 24.82]	6
	SE [bps/Hz]	4.68	1.94	[2.65, 6.71]	6
	TBLER	0.00	0.00	[0.00, 0.00]	6

TABLE IV
PERFORMANCE METRICS STATISTICAL ANALYSIS FOR PROPORTIONAL FAIR

User	Metric	Mean	Std. Dev.	95% CI	Samples
User 1	SINR [dB]	30.00	0.00	[30.00, 30.00]	93
	SE [bps/Hz]	5.50	0.50	[5.40, 5.60]	93
	TBLER	0.00	0.00	[0.00, 0.00]	93
User 2	SINR [dB]	21.12	8.08	[19.50, 22.75]	97
	SE [bps/Hz]	4.13	1.85	[3.76, 4.50]	97
	TBLER	0.15	0.06	[0.13, 0.16]	97
User 3	SINR [dB]	27.48	3.67	[26.66, 28.29]	81
	SE [bps/Hz]	5.18	1.33	[4.89, 5.48]	81
	TBLER	0.07	0.04	[0.06, 0.08]	81

D. Impact of Scheduling Algorithms and OLLA on Subcarrier Utilization

Maps showing the subcarrier and time-domain user allocation are given in Figure 11, Figure 12 and Figure 13. Under the RR algorithm (Figure 11), it can be observed that all three users appear on subcarriers with equal frequency; therefore, the spectrum is shared equally. However, it is clear from the previous metrics that this fairness is achieved at the expense of the overall efficiency of the system.

The allocation map obtained with the Best-CQI scheduler (Figure 12) shows a serious disparity between users. The vast majority of subcarriers are consistently assigned to the user with the highest SINR, while other users are excluded from the system.

In the case where the PF algorithm is applied (Figure 13), users receive resources in certain blocks over time, but in the long run, a balanced allocation profile is obtained where every user can benefit from the spectrum. This pattern demonstrates the successful implementation of a strategy that considers both channel quality utilization and user fairness.

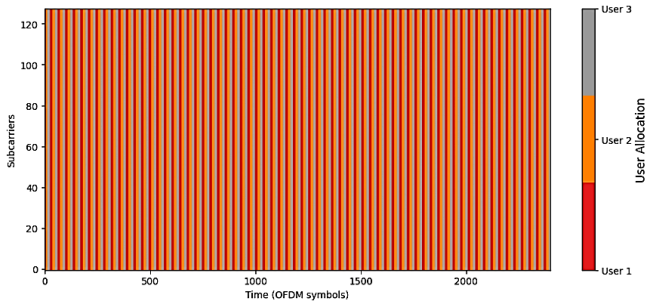

Fig. 11. Subcarrier utilization map for RR scheduler

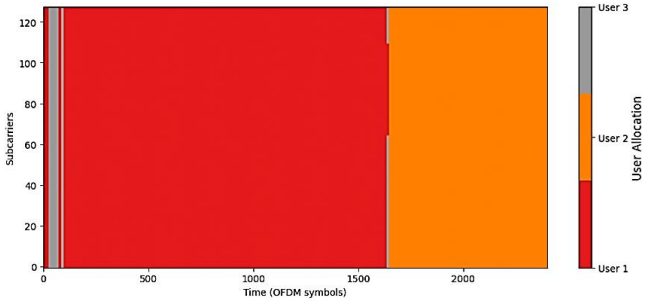

Fig. 12. Subcarrier utilization map for Best-CQI scheduler

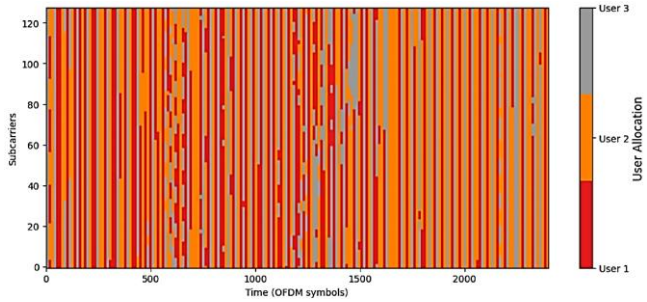

Fig. 13. Subcarrier utilization map for PF scheduler

E. Discussion

The results obtained from the simulation campaign highlight several critical insights regarding scheduler behavior and link adaptation under user mobility in a realistic wireless environment.

First, the Proportional Fair (PF) scheduler demonstrated the most balanced performance across all metrics. It achieved good spectral efficiency for all users while maintaining the achieved TBLER close to the target value of 0.1 for all users. The fairness in resource allocation, coupled with adaptive MCS selection via

OLLA, allowed PF to closely track the effective SINR variations without significant degradation in error performance.

In contrast, the Best-CQI scheduler, while achieving the highest peak spectral efficiency exceeding 5 bits/s/Hz, failed to provide reliable communication for users in low-SINR zones. The average TBLER graph for the Best-CQI algorithm shows that all users' error rates are much below 0.1. The OLLA mechanism works well in high-quality channels. This achievement applies only to resource-assignable users. Users with inadequate channel conditions often do not receive resource allocation across several time steps, preventing TBLER measurements. The Best-CQI algorithm may ignore users with low SINRs and ignore user fairness over time by relying entirely on instantaneous channel quality.

The Round Robin (RR) scheduler, on the other hand, ensured strict fairness in time-domain allocation but suffered from underutilization of spectral resources, especially in slots where users experienced poor channel conditions. Average spectral efficiency dropped below 2.5 bits/s/Hz, and OLLA had limited ability to compensate for the mismatch between allocation and instantaneous channel quality.

These relative strengths and weaknesses become even more pronounced as the number of active users increases. In denser networks these tendencies intensify: PF still apportions resources in proportion to instantaneous–average rate ratios, so it continues to balance throughput and fairness even when many users compete for the channel. Best-CQI increasingly concentrates resources on the strongest links; overall capacity rises, but the performance gap between cell-center and cell-edge users widens. RR maintains equal time sharing yet its spectral-efficiency penalty grows, because a larger share of slots is inevitably consumed by users in persistently low-SINR conditions.

A fine-grained analysis of link adaptation performance was made possible by the use of efficient SINR mapping and slot-level tracking of MCS decisions. The system's spectral efficiency, especially under PF scheduling, closely matched the theoretical Shannon limit in all cases. The dynamic interaction between SINR variation, OLLA adaptation, and selection of appropriate scheduling algorithms emerged as the key factor driving performance trends.

From an operational standpoint, the simulation findings translate into the following scheduler guidelines: In practical deployments the choice of scheduler should hinge on mobility patterns and service priorities: Proportional Fair is the best all-round candidate for heterogeneous or highly mobile cells—its instantaneous-over-average metric tracks fast SINR fluctuations while still distributing resources equitably; Best-CQI excels in capacity-driven hot spots where a few users enjoy consistently strong links (e.g., fixed-wireless access or small cells with clear LoS), maximizing aggregate throughput as long as relaxed edge-user QoS is acceptable or backed up by complementary layers; whereas coverage-oriented or strict-QoS scenarios (public-safety networks, uniformly serviced sensor clusters) benefit from the predictable airtime of Round Robin or from PF operated with a tightened fairness weight, sacrificing some spectral efficiency to guarantee that every user maintains a minimum service level.

Overall, this study looks at the connection between scheduling strategies and link adaptability under mobility in a detailed and quantitative way. It highlights how crucial it is to build balanced algorithms so that the future generation of wireless systems can handle a lot of data and be very reliable.

IV. Conclusion

This study investigates the impact of scheduling strategies on link adaptation in multi-user cellular systems using metrics such as effective SINR, spectral efficiency, and TBLER. Results show that (i) channel-agnostic Round Robin ensures airtime fairness but lowers aggregate spectral efficiency by roughly 20% relative to the Shannon limit; (ii) Best-CQI maximizes throughput, achieving within 10% of the capacity bound, yet starves low-SINR users; and (iii) Proportional Fair offers the best overall trade-off, keeping BLER close to the 10 % target while sustaining about 82% of the Shannon spectral-efficiency benchmark. Consequently, PF is preferred for mixed-mobility or QoS-balanced 6G deployments, whereas Best-CQI suits capacity-driven hot spots and RR fits coverage-oriented scenarios demanding strict airtime equity.

Future work will extend the evaluation to larger user populations and investigate reinforcement-learning schedulers that leverage short-term mobility prediction to anticipate SINR variations several slots ahead, enabling proactive MCS and resource adjustments that reduce HARQ overhead and improve latency tolerance in high-speed 6G scenarios.

References

[1] M. Elsayed and M. Erol-Kantarci, "AI-enabled future wireless networks: Challenges, opportunities, and open issues," *IEEE Vehicular Technology Magazine*, vol. 14, no. 3, pp. 70–77, 2019.

[2] T. L. Marzetta, E. G. Larsson, H. Yang, and H. Q. Ngo, *Fundamentals of massive MIMO*. Cambridge University Press, 2016.

[3] E. Peralta, G. Pocovi, L. Kuru, K. Jayasinghe, and M. Valkama, "Outer loop link adaptation enhancements for ultra reliable low latency communications in 5G," in *2022 IEEE 95th Vehicular Technology Conference:(VTC2022-Spring)*, IEEE, 2022, pp. 1–7. Accessed: July 06, 2025. [Online]. Available: https://ieeexplore.ieee.org/abstract/document/9860717.

[4] ETSI, "TS 136 213 v14.2.0, LTE;Evolved Universal Terrestrial Radio Access (E-UTRA); Physical layer procedures," (3GPP TS 36.213 version 14.2.0 Release 14), 2017.

[5] C. A. Ariyaratne, "Link Adaptation Improvements for Long Term Evolution (LTE)." 2009. Accessed: July 06, 2025. [Online]. Available: https://www.diva-portal.org/smash/record.jsf?pid=diva2:833491.

[6] Ö. Yildiz and R. I. Sokullu, "Mobility and traffic-aware resource scheduling for downlink transmissions in LTE-A systems," *Turkish Journal of Electrical Engineering and Computer Sciences*, vol. 27, no. 3, pp. 2021–2035, 2019.

[7] K. Fan, W. Chen, J. Li, X. Deng, X. Han, and M. Ding, "Mobility-aware joint user scheduling and resource allocation for low latency federated learning," in *2023 IEEE/CIC International Conference on Communications in China (ICCC)*, IEEE, 2023, pp. 1–6. Accessed: Aug. 08, 2025. [Online]. Available: https://ieeexplore.ieee.org/abstract/document/10233347.

[8] A. Deng and D. M. Blough, "Proactive Scheduling for mmWave Wireless LANs," *Computer Communications*, vol. 228, p. 107979, 2024.

[9] H. S. Sucuoglu, "Development of Real-Time Fire Detection Robotic System with Hybrid-Cascade Machine Learning Detection Structure," *Processes*, vol. 13, no. 6, p. 1712, 2025.

[10] S. Wu, C. Chakrabarti, and A. Alkhateeb, "Proactively predicting dynamic 6G link blockages using LiDAR and in-band signatures," *IEEE open journal of the communications society*, vol. 4, pp. 392–412, 2023.
[11] J. Hoydis *et al.*, "Sionna RT: Differentiable ray tracing for radio propagation modeling," in *2023 IEEE Globecom Workshops (GC Wkshps)*, IEEE, 2023, pp. 317–321. Accessed: Apr. 26, 2025. [Online]. Available: https://ieeexplore.ieee.org/abstract/document/10465179/
[12] J. Hoydis *et al.*, "Learning radio environments by differentiable ray tracing," *IEEE Transactions on Machine Learning in Communications and Networking*, 2024, Accessed: June 17, 2025. [Online]. Available: https://ieeexplore.ieee.org/abstract/document/10705152/
[13] N. Wei, A. Pokhariyal, T. B. Sørensen, T. E. Kolding, and P. E. Mogensen, "Performance of spatial division multiplexing MIMO with frequency domain packet scheduling: from theory to practice," *IEEE Journal on Selected Areas in Communications*, vol. 26, no. 6, pp. 890–900, 2008.
[14] A. A. Bin-Salem, T.-C. Wan, H. Naeem, M. Anbar, S. M. Hanshi, and A. Redjaimia, "Efficient models for enhancing the link adaptation performance of LTE/LTE-A networks," *J Wireless Com Network*, vol. 2022, no. 1, p. 10, Dec. 2022, doi: 10.1186/s13638-022-02091-w.
[15] P. Paymard, A. Amiri, T. E. Kolding, and K. I. Pedersen, "Enhanced link adaptation for extended reality code block group based HARQ transmissions," in *2022 IEEE Globecom Workshops (GC Wkshps)*, IEEE, 2022, pp. 711–716. Accessed: July 06, 2025. [Online]. Available: https://ieeexplore.ieee.org/abstract/document/10008622/
[16] Y.-J. Yu and J.-K. Wang, "NPRACH-aware link adaptation and uplink resource allocation in NB-IoT cellular networks," *IEEE Transactions on Vehicular Technology*, vol. 70, no. 5, pp. 4894–4906, 2021.
[17] R. Wang, R. Ma, G. Liu, W. Kang, W. Meng, and L. Chang, "Joint link adaption and resource allocation for satellite networks with network coding," *IEEE Transactions on Vehicular Technology*, vol. 72, no. 12, pp. 15882–15898, 2023.
[18] J. Hoydis *et al.*, "Sionna." Accessed: June 17, 2025. [Online]. Available: https://nvlabs.github.io/sionna/
[19] ITU–R P.2040–3, "Effects of building materials and structures on radiowave propagation above about 100 MHz," Geneva, 2023.
[20] K. I. Pedersen *et al.*, "Frequency domain scheduling for OFDMA with limited and noisy channel feedback," in *2007 IEEE 66th Vehicular Technology Conference*, IEEE, 2007, pp. 1792–1796. Accessed: July 10, 2025. [Online]. Available: https://ieeexplore.ieee.org/abstract/document/4350027.
[21] A. Jalali, R. Padovani, and R. Pankaj, "Data throughput of CDMA-HDR a high efficiency-high data rate personal communication wireless system," in *VTC2000-Spring. 2000 IEEE 51st Vehicular Technology Conference Proceedings (Cat. No. 00CH37026)*, IEEE, 2000, pp. 1854–1858. Accessed: July 07, 2025. [Online]. Available: https://ieeexplore.ieee.org/abstract/document/851593/

Onem YILDIZ received the B.Sc., M.Sc., and Ph.D. degrees in the Department of Electrical and Electronics Engineering from Ege University, İzmir, Türkiye, in 2014, 2017, and 2023, respectively.

She is currently serving as a Research Assistant in the Department of Electrical and Electronics Engineering at Aydın Adnan Menderes University, Aydın, Türkiye. Dr. Yıldız's research interests include wireless network optimization, mobile edge computing, resource allocation and scheduling, machine learning applications in network design, IoT-based sensing systems.